

MOL 36459

Structural Basis of Spirolactone Recognition by the Mineralocorticoid Receptor

Jessica Huyet, Grégory M. Pinon, Michel R. Fay, Jérôme Fagart, and Marie-Edith Rafestin-Oblin

INSERM, U773, Centre de Recherche Biomédicale Bichat Beaujon CRB3, BP 416, F-75018, Paris, France; Université Paris 7 Denis Diderot, site Bichat, BP 416, F-75018, Paris, France.

MOL 36459

Running title: Structural and functional characterization of MR antagonists

Address correspondence to:

Marie-Edith Rafestin-Oblin

INSERM U773, Centre de Recherche Biomédicale Bichat-Beaujon

16, rue Henri Huchard, BP416

75870 Paris, France

Tel No: (00 33) 1 44 85 63 23

Fax No: (00 33) 1 44 85 63 38

E-mail: oblin@bichat.inserm.fr

Number of text pages: **30**

Number of tables: **1**

Number of figures: **9**

Number of references: **38**

Number of words in the *Abstract*: **263**

Introduction: **635**

Discussion: **1408**

ABBREVIATIONS: 18OVP, 18-oxo-18-vinylprogesterone; DMEM, Dulbecco's minimal essential medium; GST, glutathione S-transferase; HEK, human embryonic kidney; LBD, ligand-binding domain; MMTV, mouse mammalian tumor virus; MR, mineralocorticoid receptor; RU26752, 7 α -propyl-17 α -hydroxy-3-oxopregn-4-en-21-carboxylic acid γ -lactone.

MOL 36459

ABSTRACT

Spirolactones are potent antagonists of the mineralocorticoid receptor (MR), a ligand-induced transcription factor belonging to the nuclear receptor superfamily. Spirolactones are synthetic molecules characterized by having a C17 γ -lactone, which is responsible for their antagonist character. They harbor various substituents at several positions of the steroid skeleton that modulate their potency in ways that remain to be determined. This is particularly obvious for C7 substituents. The instability of antagonist-MR complexes makes them difficult to crystallize. We took advantage of the S810L activating mutation in MR (MR_{S810L}), which increases the stability of ligand-MR complexes, to crystallize the ligand-binding domain (LBD) of MR_{S810L} associated with SC9420, a spirolactone with a C7 thioacetyl group. The crystal structure makes it possible to identify the contacts between SC9420 and MR, and elucidate the role of Met852 in the mode of accommodation of the C7 substituent of SC9420. The transactivation activities of MR_{S810L/Q776A}, MR_{S810L/R817A} and MR_{S810L/N770A} reveal that the contacts between SC9420 and the Gln776 and Arg817 residues are crucial to maintaining MR_{S810L} in its active state, whereas the contact between SC9420 and the Asn770 residue only contributes to the high affinity of SC9420 for MR. Moreover, docking experiments with other C7-substituted spirolactones revealed that the MR_{S810L}-activating potency of spirolactones is linked to the ability of their C7 substituent to be accommodated in LBD. Remarkably, the MR_{S810L}-activating and MR_{WT}-inactivating potencies of the C7-substituted spirolactones follow the same order, suggesting that the C7 substituent is accommodated in the same way in MR_{S810L} and MR_{WT}. Thus, the MR_{S810L} structure may provide a powerful tool for designing new, more effective, MR antagonists.

Introduction

Aldosterone plays a major role in regulating sodium and potassium homeostasis in tight epithelia, including the distal tubule of the kidney, the distal colon, and the salivary and sweat glands (Horisberger and Rossier, 1992; Bonvalet, 1998). It may also exert pathophysiological effects in nonepithelial target tissues, such as the adipose tissue (Penfornis *et al.*, 2000) and the cardiovascular system, where it contributes to controlling blood pressure and is implicated in some disorders, such as hypertension (Rossi *et al.*, 2005).

Aldosterone exerts its effects by binding to the mineralocorticoid receptor (MR), a ligand-activated transcription factor, which is a member of the nuclear receptor superfamily (Mangelsdorf *et al.*, 1995; Gronemeyer *et al.*, 2004). Aldosterone-dependent activation of gene transcription is thought to be a multistep process. In its ligand-free state, MR is predominantly located in the cytoplasm where it is associated with a protein complex including the heat shock protein Hsp90. When aldosterone binds to MR this induces a receptor conformation change that in turn leads to the dissociation of the associated proteins, the transfer of the complex into the nucleus, and the subsequent recruitment of transcriptional coactivators (Trapp *et al.*, 1995; Couette *et al.*, 1996; Fejes-Toth *et al.*, 1998; Hellal-Levy *et al.*, 2000; Hultman *et al.*, 2005).

Spirolactones are MR antagonists that have been widely used for the past 30 years in the treatment of sodium-retaining states and as antihypertensive agents. They improve survival in heart failure, and have beneficial effects in preventing the development of cardiac fibrosis and renal damage in patients with essential hypertension (Pitt *et al.*, 1999; Pitt *et al.*, 2003; Garthwaite and McMahon, 2004). Spirolactones are synthetic molecules with a C17 γ -lactone that is responsible for their antagonist activity, and various other substituents on the steroid skeleton that modulate their potency (Corvol *et al.*, 1977; Nickisch *et al.*, 1985; De Gasparo *et*

MOL 36459

al., 1987; Elger *et al.*, 2003; Fagart *et al.*, 2005a); this is particularly evident in the case of the C7 substituents. SC9420, a member of the spiro lactone family, characterized by having a C7 thioacetyl group, and RU26752, which has a C7 propyl group, more potently inactivate MR_{WT} than mexrenone, which harbors a C7 carboxymethyl ester group, or canrenone, which has no C7 substituent (Fagart *et al.*, 2005a). In this study, we set out to elucidate how the C7 substituent regulates the antagonist potency of spiro lactones.

The crystal structure of the ligand-binding domain (LBD) of MR when it is associated with an agonist is now available (Fagart *et al.*, 2005b; Li *et al.*, 2005; Bledsoe *et al.*, 2005). It is likely that the high stability of the agonist-MR complexes has facilitated their purification and crystallization. In contrast, the low stability of the antagonist-MR complexes (Fagart *et al.*, 1998) has made it impossible to determine the structure of the MR-LBD associated with an antagonist ligand. Interestingly, the S810L mutation, which is responsible for a severe familial form of hypertension, increases the stability of ligand-MR complexes, and switches SC9420 from an antagonist to an agonist (Geller *et al.*, 2000; Rafestin-Oblin *et al.*, 2003; Pinon *et al.*, 2004). These properties have made it possible to determine the crystal structure of MR_{S810L}-LBD associated with SC9420 (Bledsoe *et al.*, 2005). Unfortunately, the acetyl moiety of the C7 side chain is missing in this structure, and Bledsoe's report makes it clear that the ligand density ends after the sulfur atom (Bledsoe *et al.*, 2005). To characterize the anchoring of the C7 substituent of SC9420, and clarify how the C7 substituent of spiro lactones can modulate potency, we solved the crystal structure of MR_{S810L}-LBD associated with SC9420 using the same experimental conditions that we used to determine the structure of MR_{S810L}-LBD associated with progesterone and deoxycorticosterone (Fagart *et al.*, 2005b). We also elucidated the mechanism by which MR_{S810L} is activated by spiro lactones, and identified the contacts that modulate ligand affinity.

Materials and Methods

Chemicals. Aldosterone (4-pregnen-11 β ,21-diol-18-al-3,20-dione), progesterone (4-pregnen-3,20-dione) and SC9420 (7 α -acetylthio-17 β -hydroxy-3-oxopregn-4-en-21-carboxylic acid γ -lactone) were purchased from Sigma-Aldrich (St Louis, MO, USA). RU26752 (7 α -propyl-17 α -hydroxy-3-oxopregn-4-en-21-carboxylic acid γ -lactone) was kindly provided by Sanofi-Aventis (Paris, France). Canrenone was provided by Pfizer Inc. (New York, NYC, USA). Mexrenone was a gift from G. Auzou (Institut National de la Santé et de la Recherche Médicale U540, Montpellier, France). 18-oxo-18-vinylprogesterone (18-vinyl-4-pregnen-3,18,20-trione; 18OVP) was a gift from A. Marquet (Paris, France). All other products used in the biochemical studies were purchased from Sigma-Aldrich (St Louis, MO, USA).

Expression Vectors. The expression vector pchMR_{WT} contains the entire coding sequence of wild-type human MR (Fagart *et al.*, 1998). The expression vectors pchMR_{N770A}, pchMR_{S810L}, pchMR_{S810L/Q776A} and pchMR_{S810L/R817A} contain the coding sequences of mutant MR_{N770A}, MR_{S810L}, MR_{S810L/Q776A} and MR_{S810L/R817A}, respectively (Fagart *et al.*, 1998; Rafestin-Oblin *et al.*, 2003; Fagart *et al.*, 2005b). The expression vector pchMR_{S810L/N770A} was created by cutting out the Bpu1102I-AflIII fragment from pchMR_{S810L} and inserting it into pchMR_{N770A}. The plasmid pc β gal contains the coding sequence for the β -galactosidase (Fagart *et al.*, 2005a). The plasmid pFC31Luc contains the MMTV promoter that drives the luciferase gene (Gouilleux *et al.*, 1991). The expression vector pMRLBDL810 contains the coding sequence for the fusion protein between GST and MR-LBD that harbors the S810L and C910A mutations (Fagart *et al.*, 2005b).

Protein Expression and Purification. Fermentation using the BL21 CodonPlus (DE3) RIL strain from Stratagene (Amsterdam, The Netherlands) transformed with the

MOL 36459

pMRLBDL810 vector was carried out in the presence of 100 μ M SC9420. Expression was induced by incubating with 200 μ M isopropyl- β -D-thiogalactoside (IPTG) for 16 h at 15°C. After centrifuging, the bacteria were disrupted by sonication in TENG buffer (50 mM Tris-HCl pH 7.5, 150 mM NaCl, 5 mM EDTA, 10% glycerol, 0.1% n-octyl- β -glucoside (NOG)) supplemented with 100 μ M SC9420. The lysate was clarified and loaded onto a GStrap column (Amersham, Les Ulis, France). The fusion protein was eluted with 15 mM of reduced glutathione in the TENG buffer. After diluting the eluate to a protein concentration of 1 mg/ml, the fusion protein was cleaved by exposing to thrombin protease (20 units/mg of fusion protein) overnight at 4°C. The protein mixture was diluted a further 5-fold in a HENG buffer (10 mM HEPES pH 6.8, 10% glycerol, 0.1% NOG) supplemented with 100 μ M SC9420, loaded onto a sulfoxide column (SP XL from Amersham, Les Ulis, France), and eluted with a gradient of 0-500 mM NaCl in the HENG buffer. The fractions containing the LBD were pooled and concentrated to a protein concentration of 7 mg/ml.

Crystallization and Data Collection. Crystals were grown over few days at room temperature in hanging drops containing 1 μ l of protein solution and 1 μ l of well buffer (100 mM HEPES pH 6.8, 230 mM NaCl, 25% PEG 4000). Before data collection, the crystals were flash frozen in liquid nitrogen without adding any cryoprotecting agent. Diffraction data were collected to a resolution of 2.29 Å, at a temperature of -80.1°C and at a wavelength of 0.979707 Å on the FIP-BM30A beamline at the European Synchrotron Radiation Facility (ESRF, Grenoble, France) using a MarCCD detector. The data set was integrated and scaled using XDS (Kabsch *et al.*, 1993).

Structure Determination and Refinement. The crystal structure was determined by molecular replacement, using Phaser (Storoni *et al.*, 2004) with the coordinates of the MR_{S810L}-LBD associated with deoxycorticosterone (PDB ID 1Y9R; Fagart *et al.*, 2005b) as the search model. The complex crystallized in the P3₂ space group. From molecular

MOL 36459

replacement, two rotation solutions clearly appeared, and three translation solutions were obtained for each of these rotation solutions, indicating the presence of six molecules in the asymmetric unit. Several rounds of manual rebuilding using the SigmaA weighted 2 Fo-Fc electron density maps, followed by simulated annealing and individual isotropic B factor refinements were performed using CNS (Brunger *et al.*, 1998). Solvent molecules were located in a Fo-Fc map contoured at 2σ . The final R and R-free values were 24% and 26.3%, respectively. The final model was validated with PROCHECK (Laskowski *et al.*, 1993), 99.7% of the residues lie within the allowed regions of the Ramachandran Plot.

Determination of the cavity volumes. The volume of the ligand-binding cavity of MR_{S810L}, associated with SC9420, and that of MR_{S810L}, associated with progesterone, were calculated using the probe-occupied algorithm of the VOIDOO package (Kleywegt and Jones, 1994). This algorithm uses a probe-sphere of 1.4 Å radius. The contacts between the probe-sphere and the van der Waals protein surface delineate the probe-occupied cavity. The volume of the ligand-binding cavity of MR_{S810L}, associated with SC9420, and that of MR_{S810L}, associated with progesterone, were calculated for each monomer of the asymmetric unit. The values reported in the Results section are the means of the monomer volumes.

Docking Experiments. RU26752 and mexrenone were constructed and minimized using the InsightII package (Accelrys, Cambridge, UK). Both spiro lactones were manually docked within the crystal structure of the MR_{S810L}-LBD associated with SC9420 using the O package (Jones *et al.*, 1991).

Cells Culture and Transfection Procedures. HEK 293T cells were cultured in high-glucose-containing DMEM (Invitrogen, Cergy Pontoise, France), 25 mM HEPES, 2x non-essential amino acids, 2 mM glutamine, 100 IU/ml penicillin and 100 µg/ml streptomycin, supplemented with 10% heat-inactivated fetal calf serum (FCS) at 37°C in a humidified atmosphere and with 5% CO₂. Four hours before transfection, the cells were cultured in the

MOL 36459

same medium supplemented with 10% charcoal-treated FCS. Transfections were carried out using the calcium phosphate precipitation method. Cells were transfected with 2 μg of one of the receptor expression vectors (pchMR_{WT}, pchMR_{N770A}, pchMR_{S810L}, pchMR_{S810L/N770A}, pchMR_{S810L/Q776A} or pchMR_{S810L/R817A}), 7 μg pFC31Luc and 1 μg pc β gal in 1x HEPES-buffered saline supplemented with 160 mM CaCl₂. Twelve hours after transfection, the cells were rinsed with PBS, trypsinized and replated in twelve-well plates. The steroids to be tested were added to the cells 24 h after seeding. After incubating for 24 h, cell extracts were assayed for luciferase and β -galactosidase activities (De Wet *et al.*, 1987; Herbomel *et al.*, 1984). To standardize the transfection efficiency, the relative light units obtained in the luciferase assay were divided by the optical density obtained in the β -galactosidase assay. Each point is the mean \pm SEM of three separate experiments.

MOL 36459

Results

Effects of the C7 Substituent of Spirolactones on the Agonist Activity of MR_{S810L}. It has been reported that SC9420, a spirolactone with a C7 thioacetyl group, activates the MR carrying the S810L mutation (MR_{S810L}) (Geller *et al.*, 2000). We wondered whether spirolactones lacking C7 substituent (canrenone) or harboring a C7 substituent distinct from that of SC9420 (RU26752 and mexrenone, see formulae Fig. 1), are also able to activate MR_{S810L}. We investigated the ability of these spirolactones to activate MR_{S810L} transiently expressed in HEK293T cells. Transfection assays performed with pchMR_{S810L} revealed that RU26752, which is characterized by having a C7 propyl group, activates MR_{S810L} as potently as SC9420, and has an ED₅₀ value of $\sim 10^{-10}$ M, close to that of aldosterone (ED₅₀ $\sim 5 \times 10^{-11}$ M) (Fig. 2). Mexrenone, with a C7 carboxymethyl ester group, is less potent than SC9420 (ED₅₀ $\sim 10^{-9}$ M) (Fig. 2). Canrenone, which has no C7 substituent, displays lower agonist activity corresponding to $\sim 60\%$ of the maximum aldosterone-induced MR_{S810L} activity (Fig. 2), and has no antagonist activity (data not shown). Thus, all the spirolactones tested activate MR_{S810L}, and their potencies depend on the C7 substituents. Interestingly, the MR_{S810L}-activating and MR_{WT}-inactivating (Fagart *et al.*, 2005a) potencies of the C7-substituted spirolactones follow the same order, suggesting that the C7 substituent is accommodated in the same way in MR_{S810L} and MR_{WT}.

Crystal Structure of the Ligand-Binding Domain of MR_{S810L} Associated with SC9420.

To identify the accommodation mode of SC9420 within the ligand-binding cavity of MR, we solved the crystal structure of the LBD of MR_{S810L} associated with SC9420. The MR_{S810L}-LBD was expressed as a fusion protein with glutathione S-transferase (GST) in the presence of a high concentration of SC9420, and then purified according to the protocol previously described (Fagart *et al.*, 2005b). Briefly, the fusion protein was purified by affinity

MOL 36459

chromatography, and cleaved by the action of the thrombin protease. The LBD was separated from GST by cation exchange chromatography, and then crystallized by the vapor diffusion method. The structure was solved by molecular replacement, using the crystal structure of MR_{S810L}-LBD associated with deoxycorticosterone as a template (PDB ID 1Y9R; Fagart *et al.*, 2005b), and was then refined to 2.3 Å resolution (see Table 1). The complex crystallized in the P3₂ space group with six molecules in the asymmetric unit (see Table 1). MR_{S810L}-LBD associated with SC9420 is composed of 11 α-helices (H1, H3-H12), and two short β-sheets, organized into three layers. The quality of the density map made it possible to pinpoint the position of SC9420 accurately in the ligand-binding cavity (Fig. 3A). This cavity is lined by 22 residues, five of which are polar, and three anchor the ligand (Fig. 3B). The C3 ketone function of SC9420 is hydrogen bound to the Gln776 and Arg817 residues and to a water molecule (Fig. 3B). The ketone function of the C17 γ-lactone of SC9420 establishes a hydrogen bond with the Asn770 residue (Fig. 3B). Seventeen residues contribute to the hydrophobic nature of the binding cavity, and stabilize the position of SC9420 through numerous van der Waals contacts (Fig. 3B). The Leu810 residue forms short hydrophobic contacts with the C19 methyl group of SC9420, and with the Gln776 residue (Fig. 3, A and B). The C7 thioacetyl group of SC9420 is clearly defined in the electron density map (Fig. 3A). It is accommodated within a small hydrophobic groove delimited by Ser811 (H5), Leu814 (H5), Leu827 (β-turn), Phe829 (β-turn), Met845 (H7), Cys849 (H7), Met852 (H7) and Leu938 (H11) (Fig. 3B), where it establishes numerous van der Waals contacts.

We next compared the crystal structure of MR_{S810L}, associated with SC9420, with that of MR_{S810L}, associated with progesterone, a ligand with no C7 substituent (PDB ID 1YA3; Fagart *et al.*, 2005b). The orientations of the Ser811, the Met845 and the Met852 residue side chains of the ligand-binding cavity are modified (compare Fig. 4A and B). The slight changes in the orientation of the Ser811 and the Met845 residues side chains modify neither the van

MOL 36459

der Waals volume occupied by these residues, nor the volume of the ligand-binding cavity. In contrast, changing the orientation of the Met852 residue has a drastic impact. Its side chain adopts a folded back conformation in the presence of the C7-substituted SC9420 (Fig. 4A) that is different from the extended conformation observed with progesterone, a steroid with no C7 substituent (Fig. 4B). Accordingly, the volume of the ligand-binding cavity of MR_{S810L} associated with SC9420 is larger than that of MR_{S810L} associated with progesterone (499 Å³ vs 406 Å³) (Fig. 4, A and B). Thus, the presence of the C7 thioacetyl group of SC9420 modifies the conformation of the Met852 side chain, creating a small groove within which the C7 substituent is accommodated and establishes numerous contacts.

Finally, we compared the crystal structure of MR_{S810L}, associated with SC9420, and that of MR_{WT}, associated with deoxycorticosterone, a molecule that activates both MR_{WT} and MR_{S810L} (PDB ID 2ABI). Superimposing the two structures reveals that the overall organization of the two structures is very similar, the positioning of all eleven helices being the same (Fig. 5A). Superimposing the ligand-binding cavity of MR_{S810L}, associated with SC9420, over that of MR_{WT}, associated with deoxycorticosterone, shows that the Leu810 residue establishes short hydrophobic contacts with the C19 methyl group of SC9420, and with the Gln776 residue (Fig. 5B). The superimposition of the two structures also reveals that the network of contacts, created by the Leu810 residue, does not exist in the MR_{WT} (Fig. 5B). Thus, the S810L mutation does not modify the overall organization of the receptor, but does allow additional contacts to occur that stabilize the receptor in its active state.

C7-Substituted Spirolactones Docking within the MR_{S810L}-LBD. To find out how the C7 side chain of RU26752 and mexrenone can be accommodated within the ligand-binding cavity, we determined the lowest energy conformation of the C7 substituents of spirolactones by performing phi/psi rotation searches, and docked these molecules within the structure of MR_{S810L}-LBD associated with SC9420. The orientation of the thioacetyl group of SC9420

MOL 36459

determined by the lowest energy conformation search is the same as that observed in the crystal structure, suggesting that no modification of the C7 substituent orientation occurs when SC9420 binds to MR_{S810L} (Fig. 6A). The minimized conformations search reveals that the propyl group of RU26752 is oriented in the same way as the thioacetyl group of SC9420, and docking experiments show that it fits well into the groove created by the folded back conformation of the Met852 residue, where it establishes numerous contacts (Fig. 6B). In contrast, the minimization of mexrenone shows that the orientation of its C7 side chain is different from that of SC9420. The docking experiment of the minimized mexrenone within the crystal structure of MR_{L810}-LBD associated with SC9420 reveals that its C7 substituent is too close to the Phe829 and the Leu938 residues, leading to unfavorable contacts (Fig. 6C). The rotation of the C7 side chain would be possible, but would necessitate energy consuming adaptation of the receptor and/or of mexrenone. Thus, the accommodation mode of the C7 substituent of spirolactones is directly linked to their structure.

Activation Mechanism of the MR_{S810L} by Spirolactones. The structure revealed that SC9420 is anchored by several hydrogen bonds, between the C3 ketone function and the Gln776 and the Arg817 residues and between the C17 γ -lactone and the Asn770 residue. The question arose of which contacts are involved in stabilizing spirolactone-MR_{S810L} in its active state. To identify these contacts, we replaced the polar residues Asn770, Gln776 or Arg817 by an alanine within MR_{S810L}, and then tested the ability of spirolactones with various C7 substituent to activate the corresponding double-mutant receptors (MR_{S810L/N770A}, MR_{S810L/Q776A} and MR_{S810L/R817A}). Transfection assays performed with pchMR_{S810L/Q776A} and pchMR_{S810L/R817A} showed that all the spirolactones tested were unable to activate MR_{S810L/Q776A} and MR_{S810L/R817A} (data not shown), which contrasted with their ability to activate MR_{S810L}. The next question was whether spirolactones act as antagonist ligands when bound to MR_{S810L/Q776A} and MR_{S810L/R817A}. To answer this question, HEK 293T cells

MOL 36459

transiently expressing MR_{S810L/Q776A} or MR_{S810L/R817A} were incubated with aldosterone, in the presence of rising concentrations of spiro lactones. Aldosterone has been reported to activate MR_{S810L/Q776A} and MR_{S810L/R817A} with ED₅₀ values of $\sim 10^{-7}$ and 10^{-8} M, respectively (Fagart *et al.*, 2005). RU26752 and SC9420 inhibit the aldosterone-induced transactivation activities of MR_{S810L/Q776A} and MR_{S810L/R817A} in a dose-dependent manner with IC₅₀ values ranging from 1 to 5×10^{-7} M (Fig. 7, A and B). Mexrenone and canrenone also inhibited the aldosterone-induced transactivation activities of MR_{S810L/Q776A} and MR_{S810L/R817A} but with less potency, their IC₅₀ values ranging from 5 to 10×10^{-6} M (Fig. 7, A and B). Thus, the Q776A and the R817A mutations within MR_{S810L} abolish the agonist character that spiro lactones display when bound to the MR_{S810L}. In addition, the potency of spiro lactones for inactivating MR_{S810L/Q776A} and MR_{S810L/R817A} follows the same order as that for activating MR_{S810L} (RU26752 > SC9420 > mexrenone > canrenone). Overall, these findings indicate that the S810L mutation stabilizes the spiro lactone-receptor complexes in their active state, by reinforcing their contacts with the Gln776 and the Arg817 residues without modifying their potencies.

We then investigated the role of the Asn770 residue in MR_{S810L} activation by spiro lactones. Progesterone activated MR_{S810L/N770A} with an ED₅₀ value of $\sim 5 \times 10^{-9}$ M, but aldosterone did not (data not shown). We therefore used progesterone as an agonist ligand in the transfection assays performed with pchMR_{S810L/N770A}. At a concentration of 10^{-5} M, RU26752 induced 60% of the maximum progesterone-induced MR_{S810L/N770A} activity (Fig. 8A). At the same concentration, SC9420, mexrenone and canrenone activate MR_{S810L/N770A} by 13%, 10% and 3%, respectively (Fig. 8A). The question then arose as to whether spiro lactones would display antagonist properties when bound to MR_{S810L/N770A}. Transfection assays performed with pchMR_{S810L/N770A} revealed that at a concentration of 10^{-5} M, SC9420 inhibited progesterone-induced MR_{S810L/N770A} activity by 75%, whereas RU26752, mexrenone and canrenone

MOL 36459

antagonized the effects of progesterone by only 11%, 29% and 27%, respectively (Fig. 8B). Spirolactones modified the transactivation properties of MR_{S810L/N770A} only at a high concentration (10^{-5} M). As the N770A mutation within MR_{S810L} dramatically reduced the ability of spirolactones both to activate and inactivate the receptor, it seems likely that it must play a key role in the affinity of spirolactones for MR_{S810L}.

Role of the Asn770 Residue in MR_{WT}. It has been reported that the antagonist character of spirolactones when bound to the MR_{WT} is due to their inability to establish contact with the Asn770 residue (Fagart *et al.*, 1998). We observed here that the contact between spirolactones and the Asn770 residue is important for their high affinity for MR_{S810L}. This led us to wonder whether the Asn770 residue also contributes to the high affinity of spirolactones for MR_{WT}. The Asn770 residue was replaced by an alanine in the context of the wild-type receptor, and the ability of the corresponding mutant MR_{N770A} to be inactivated by spirolactones was tested and compared to that of MR_{WT}. The synthetic compound 18-oxo-18-vinylprogesterone (18OVP) was used in the transfection assays as it is able to activate both MR_{WT} and MR_{N770A} with the same potency (ED₅₀ values of $\sim 5 \times 10^{-8}$ M) (Souque *et al.*, 1995; Fagart *et al.*, 1998). SC9420, RU26752, mexrenone and canrenone very potently inhibited the MR_{WT} activity induced by 18OVP (Fig. 9A). Complete inhibition was observed for a concentration of spirolactones of 10^{-6} M (Fig. 9A). Following the N770A mutation within MR_{WT}, all the spirolactones retained their antagonist character, but they displayed lower potency (Fig. 9B). At 10^{-6} M, SC9420, mexrenone and canrenone inhibited the 18OVP-induced MR_{N770A} activity by 20-45%, compared to more than 90% inhibition of the MR_{WT} (Fig. 9B). The antagonist potency of RU26752 was also decreased, but to a lesser extent. Indeed, at a concentration of 10^{-7} M, RU26752 inhibited the 18OVP-induced activity of MR_{WT} and MR_{N770A} by 90% and 40%, respectively (Fig. 9B). Thus, it can be suggested that the Asn770 residue may play a key role in the affinity of spirolactones for MR_{WT}.

Discussion

The present study shows that spiro lactones activate the MR harboring the S810L mutation, which is responsible for hypertension, whereas they act as antagonists when bound to the wild-type receptor. It also indicates that the potencies of spiro lactones in activating MR_{S810L} and inactivating MR_{WT} follow the same order, allowing us to propose that the contacts involved in MR_{S810L}-activation by spiro lactones may be different from those that modulate their potency.

The understanding of the activation mechanism of nuclear receptors has been greatly improved by crystallographic studies of LBDs in their inactive and active states. The LBD of nuclear receptors that surrounds the ligand-binding cavity is rather dynamic, and exhibits some of the properties of a molten globule in the absence of ligand (Nagy and Schwabe, 2004). Binding a ligand compacts the LBD by establishing many polar and hydrophobic contacts. Some of these are involved in the stability of the ligand-receptor complex, and others are required to stabilize the complex in its active state, facilitating the recruitment of transcriptional coactivators (Nagy and Schwabe, 2004). Several structures of the LBD of MR in its agonist conformation are now available (Fagart *et al.*, 2005; Bledsoe *et al.*, 2005; Li *et al.*, 2005). In contrast, no structure of MR in its apo and antagonist conformation is yet available, making it impossible to identify the conformational changes that take place in response to agonist or antagonist binding. Nevertheless, a few years ago, it was shown that the contact between the Asn770 residue of MR_{WT} and the C21 hydroxyl function of aldosterone, or the C11 hydroxyl function of 11 β -hydroxyprogesterone, is responsible for the agonist character of these molecules (Fagart *et al.*, 1998; Rafestin-Oblin *et al.*, 2002). In contrast, the MR antagonists, such as progesterone or spiro lactones, are unable to contact the Asn770 residue (Fagart *et al.*, 1998). Thus, the mechanism by which antagonist ligands inactivate the

MOL 36459

MR is based on the instability of the antagonist-MR complexes, rather than on the ability of the antagonist ligand to stabilize the MR in an inactive state, favoring the recruitment of corepressors (Fagart *et al.*, 1998).

In this study, transactivation experiments revealed that spirolactones activate MR, harboring the S810L mutation (MR_{S810L}). These results raised the question of how the S810L mutation modifies spirolactone-receptor contacts, allowing MR_{S810L} to be maintained in its active state. The crystal structure of the MR_{S810L}-LBD associated with SC9420 reported here reveals that the domain is composed of 11 α -helices (H1, H3-H12) and two short β -sheets, organized into three layers. The H12 helix is folded back toward the core of the domain, closing the ligand-binding pocket. The C-terminal extension is anchored to the region delineated by H8, H9 and H10 helices, by numerous van der Waals contacts and by hydrogen bonds. This overall organization is similar to that of MR in its active state (Fagart *et al.*, 2005b; Li *et al.*, 2005; Bledsoe *et al.*, 2005). Thus, the S810L mutation does not modify the positioning of the helices of the LBD. The H12 helix, which plays a crucial role in the activation process of the steroid receptors, adopts the same position in MR_{WT} and MR_{S810L}. This finding suggests that agonist binding to MR_{WT} and MR_{S810L} leads to the recruitment of transcriptional coactivators that occurs in a similar way.

The crystal structure of MR_{S810L}-LBD associated with SC9420 reveals that the Leu810 residue establishes short hydrophobic contacts with the C19 methyl of SC9420 and the Gln776 residue, which do not exist in MR_{WT}. It also reveals that SC9420 is anchored by the Gln776 and the Arg817 residues, and also by the Asn770 residue. This last contact was remarkable, since MR_{WT}-inactivation by spirolactones is based on the absence of contact between the Asn770 residue and spirolactones (Fagart *et al.*, 1998). This led us to wonder about the contribution made by each of the contacts between spirolactones and the polar residues Asn770, Gln776 and Arg817 to the process of MR_{S810L} activation. Mutagenesis

MOL 36459

analysis revealed that the ability of spiro lactones to modulate the MR_{S810L}-activity is dramatically reduced by the N770A mutation. Thus, within MR_{S810L}, the contact between the Asn770 residue and spiro lactones is not crucial for stabilizing MR_{S810L} in its active state, but it does play a key role in the affinity of spiro lactones. Interestingly, steroids harboring a C11 hydroxyl group, such as 11 β -hydroxyprogesterone and cortisol, or a C11-C18 hemiketal group, as aldosterone, are not able to activate MR_{S810L/N770A} to a significant degree (Bledsoe *et al.*, 2005). Only progesterone and deoxycorticosterone, which have no C11 substitution, are able to activate MR_{S810L/N770A} (Bledsoe *et al.*, 2005). Overall, these results show clearly that, in the context of MR_{S810L}, the anchoring of steroids having a C11 hydroxyl function or a C17 γ -lactone involves the Asn770 residue.

We wondered whether the two other polar residues Gln776 and Arg817, which anchor the C3 ketone function of spiro lactones, play any role in stabilizing spiro lactone-MR_{S810L} complexes in their active state. The replacement of the Gln776 or Arg817 residue by an alanine within MR_{S810L} abolishes their agonist character, and restores the antagonist character that spiro lactones display when bound to MR_{WT}. Furthermore, the potencies of spiro lactones in inactivating MR_{WT}, MR_{S810L/Q776A} and MR_{S810L/R817A} and activating MR_{S810L} follow the same order. This suggests that the contacts involving the Gln776 and Arg817 residues play a minor role in modulating the affinity of spiro lactones for MR_{S810L}, but are crucial for the activation of MR_{S810L} by spiro lactones. Thus, the S810L mutation within MR reinforces the contacts between the C3 ketone function of spiro lactones and the Gln776 and the Arg817 residues; each of these contacts becomes crucial for stabilizing the spiro lactone-MR_{S810L} complexes in their active state. The activation of MR_{S810L} by progesterone also requires strong stabilizing contacts implicating the Gln776 and the Arg817 residues, whereas these contacts are dispensable for the activation of MR_{S810L} by C21-hydroxylated compounds, such as aldosterone and deoxycorticosterone (Fagart *et al.*, 2005b). Thus, the Gln776 and the Arg817

MOL 36459

residues are implicated in the mechanism of MR_{S810L} activation by steroids harboring a ketone function at the C3 position, but with no C21 hydroxyl function. These findings are consistent with the antagonist property of the synthetic ligand 5 α -pregnane-20-one that is unable to contact the Gln776 and the Arg817 residues, due to the absence of a C3 ketone function (Pinon *et al.*, 2004).

Interestingly, we observed that MR_{S810L}-activating potency of spiro lactones depends on their C7 substituents. The structure reported here reveals that the side chain of the Met852 residue, a residue facing the C7 substituent of SC9420, adopts a folded back conformation. In all the currently reported structures of MR-LBD associated with a ligand without the C7 substituent, the side chain of the Met852 residue adopts an extended conformation (Fagart *et al.*, 2005b; Li *et al.*, 2005; Bledsoe *et al.*, 2005). This makes it likely that molecular adaptation of the side chain of the Met852 residue may be required to accommodate ligands with a C7 substituent. The folded back conformation of the Met852 residue side chain creates a small groove surrounded by several hydrophobic residues. The C7 thioacetyl group of SC9420 fits well into this groove, where it makes numerous stabilizing van der Waals contacts. These contacts are responsible for the high MR_{S810L}-activating potency of SC9420. Docking experiments revealed that the C7 propyl group of RU26752 is accommodated in a similar way to the C7 thioacetyl group of SC9420, whereas the C7 carboxymethyl ester group of mexrenone induces steric hindrance with the Phe829 residue. Thus, the accommodation of the C7 substituent within the ligand-binding cavity correlates well with the MR_{S810L}-activating potency of C7-substituted spiro lactones.

In conclusion, mutagenesis analyses based on the crystal structure of MR_{S810L}-LBD associated with SC9420, combined with docking experiments, make it possible to distinguish the residues responsible for the MR_{S810L} activation from those that modulate the ligands affinity. The contacts involving the Gln776 and the Arg817 residues are crucial for the

MOL 36459

activation of MR_{S810L} by spiro lactones, whereas the Asn770 and the Met852 residues are key modulators of the affinity of spiro lactones for MR_{S810L}. Another important conclusion of the study is that spiro lactones also contact the Asn770 residue in MR_{WT}. This contact is not strong enough to stabilize the complex in its active state, but is involved in the affinity of spiro lactones for MR_{WT}. Since the MR_{S810L}-activating potencies of spiro lactones correlate with their potencies in inactivating MR_{WT}, it can be surmised that the C7 substituents are accommodated in same way in MR_{WT} as in MR_{S810L}. Thus, the crystal structure of MR_{S810L} may provide a powerful tool for designing new, more effective, C7-substituted MR antagonists.

MOL 36459

Acknowledgements

We would like to thank M. Pirocchi and J.-L. Ferrer from the FIP-BM30A beamline at the European Synchrotron Radiation Facilities for assistance with data collection. We are also grateful to H. Richard-Foy and F. Gouilleux for providing plasmid pFC31Luc. We also thank colleagues for their critical reading of the manuscript.

MOL 36459

References

- Bledsoe RK, Madauss KP, Holt JA, Apolito CJ, Lambert MH, Pearce KH, Stanley TB, Stewart EL, Trump RP, Willson TM, and Williams SP (2005) A ligand-mediated hydrogen bond network required for the activation of the mineralocorticoid receptor. *J Biol Chem* **280**:31283-31293.
- Bonvalet JP (1998) Regulation of sodium transport by steroid hormones. *Kidney Int Suppl* **65**:49-56.
- Brunger AT, Adams PD, Clore GM, DeLano WL, Gros P, Grosse-Kunstleve RW, Jiang JS, Kuszewski J, Nilges M, Pannu NS, Read RJ, Rice LM, Simonson T, and Warren GL (1998) Crystallography and NMR system: A new software suite for macromolecular structure determination. *Acta Crystallogr D Biol Crystallogr* **54**:905-921.
- Corvol P, Claire M, Rafestin-Oblin ME, Michaud A, Roth-Meyer C, and Menard J (1977) Spirolactones: clinical and pharmacologic studies. *Adv Nephrol Necker Hosp* **7**:199-215.
- Couette B, Fagart J, Jalaguier S, Lombes M, Souque A, and Rafestin-Oblin ME (1996) Ligand-induced conformational change in the human mineralocorticoid receptor occurs within its hetero-oligomeric structure. *Biochem J* **315**:421-427.
- De Gasparo M, Joss U, Ramjoue HP, Whitebread SE, Haenni H, Schenkel L, Kraehenbuehl C, Biollaz M, Grob J, and Schmidlin J (1987) Three new epoxy-spirolactone derivatives: characterization in vivo and in vitro. *J Pharmacol Exp Ther* **240**:650-656.
- De Wet JR, Wood KV, Deluca M, Helinski DR, and Subramani S (1987) Firefly luciferase gene: structure and expression in mammalian cells. *Mol Cell Biol* **7**:725-737.
- Elger W, Beier S, Pollow K, Garfield R, Shi SQ, and Hillisch A (2003) Conception and pharmacodynamic profile of drospirenone. *Steroids* **68**:891-905.
- Fagart J, Wurtz JM, Souque A, Hellal-Levy C, Moras D, and Rafestin-Oblin ME (1998) Antagonism in the human mineralocorticoid receptor. *EMBO J* **17**:3317-3325.

MOL 36459

- Fagart J, Seguin C, Pinon GM, and Rafestin-Oblin ME (2005a) The Met852 residue is a key organizer of the ligand-binding cavity of the human mineralocorticoid receptor. *Mol Pharmacol* **67**:1714-1722.
- Fagart J, Huyet J, Pinon GM, Rochel M, Mayer C, and Rafestin-Oblin ME (2005b) Crystal structure of a mutant mineralocorticoid receptor responsible for hypertension. *Nat Struct Mol Biol* **12**:554-555.
- Fejes-Toth G, Pearce D, and Naray-Fejes-Toth A (1998) Subcellular localization of mineralocorticoid receptors in living cells: effects of receptor agonists and antagonists. *Proc Natl Acad Sci USA* **95**:2973-2978.
- Garthwaite SM and McMahon EG (2004) The evolution of aldosterone antagonists. *Mol Cell Endo* **217**:27-31.
- Geller DS, Farhi A, Pinkerton N, Fradley M, Moritz M, Spitzer A, Meinke G, Tsai FT, Sigler PB, and Lifton RP (2000) Activating mineralocorticoid receptor mutation in hypertension exacerbated by pregnancy. *Science* **289**:119-123.
- Gouilleux F, Sola B, Couette B, and Richard-Foy H (1991) Cooperation between structural elements in hormone-regulated transcription from the mouse mammary tumor virus promoter. *Nucleic Acids Res* **19**:1563-1569.
- Gronemeyer H, Gustafsson JA, and Laudet V (2004) Principles for modulation of the nuclear receptor superfamily. *Nat Rev Drug Discov* **3**:950-964.
- Hellal-Levy C, Fagart J, Souque A, and Rafestin-Oblin ME (2000) Mechanistic aspects of mineralocorticoid receptor activation. *Kidney Int* **57**:1250-1255.
- Herbomel P, Bourachot B, and Yaniv M (1984) Two distinct enhancers with different cell specificities coexist in the regulatory region of polyoma. *Cell* **39**:653-662.
- Horisberger JD and Rossier BC (1992) Aldosterone regulation of gene transcription leading to control of ion transport. *Hypertension* **19**:221-227.

MOL 36459

- Hultman ML, Krasnoperova NV, Li S, Du S, Xia C, Dietz JD, Lala DS, Welsch DJ, and Hu X (2005) The ligand-dependent interaction of mineralocorticoid receptor with coactivator and corepressor peptides suggests multiple activation mechanisms. *Mol Endocrinol* **19**:1460-1473.
- Jones TA, Zou JY, Cowan SW, and Kjeldgaard M (1991) Improved methods for building protein models in electron density maps and the location of errors in these models. *Acta Crystallogr A* **47**:110-119.
- Kabsch W (1993) Automatic processing of rotation diffraction data from crystals of initially unknown symmetry and cell constants. *J Appl Cryst* **26**:795-800.
- Kleywegt GJ and Jones TA (1994) Detection, delineation, measurement and display of cavities in macromolecular structures. *Acta Crystallogr D Biol Crystallogr* **50**:178-185.
- Laskowski RA, MacArthur MW, Moss DS, and Thornton JM (1993) PROCHECK: a program to check the stereochemical quality of protein structures. *J Appl Cryst* **26**:283-291.
- Li Y, Suino K, Daugherty J, and Xu HE (2005) Structural and biochemical mechanisms for the specificity of hormone binding and coactivator assembly by mineralocorticoid receptor. *Mol Cell* **19**:367-380.
- Mangelsdorf DJ, Thummel C, Beato M, Herrlich P, Schutz G, Umesono K, Blumberg B, Kastner P, Mark M, Chambon P, and Evans RM (1995) The nuclear receptor superfamily: the second decade. *Cell* **83**:835-839.
- Nagy L and Schwabe JW (2004) Mechanism of the nuclear receptor molecular switch. *Trends Biochem Sci* **29**:317-324.
- Nickisch K, Bittler D, Casals-Stenzel J, Laurent H, Nickolson R, Nishino Y, Petzoldt K, and Wiechert R (1985) Aldosterone antagonists. 1. Synthesis and activities of 6 beta,7 beta:15 beta,16 betadimethylene steroidal spirolactones. *J Med Chem* **28**:546-550.

MOL 36459

Penformis P, Viengchareun S, Le Menuet D, Cluzeaud F, Zennaro MC, and Lombes M (2000)

The mineralocorticoid receptor mediates aldosterone-induced differentiation of T37i cells into brown adipocytes. *Am J Physiol Endocrinol Metab* **279**:386-394.

Pinon GM, Fagart J, Souque A, Auzou G, Vandewalle A, and Rafestin-Oblin ME (2004)

Identification of steroid ligands able to inactivate the mineralocorticoid receptor harboring the S810L mutation responsible for a severe form of hypertension. *Mol Cell Endo* **217**:181-188.

Pitt B, Zannad F, Remme WJ, Cody R, Castaigne A, Perez A, Palensky J, and Wittes J (1999)

The effect of spironolactone on morbidity and mortality in patients with severe heart failure. Randomized Aldactone Evaluation Study Investigators. *N Engl J Med* **341**:709-717.

Pitt B, Remme W, Zannad F, Neaton J, Martinez F, Roniker B, Bittman R, Hurley S, Kleiman

J, and Gatlin M; Eplerenone Post-Acute Myocardial Infarction Heart Failure Efficacy and Survival Study Investigators (2003) Eplerenone, a selective aldosterone blocker, in patients with left ventricular dysfunction after myocardial infarction. *N Engl J Med* **348**:1309-1321.

Rafestin-Oblin ME, Fagart J, Souque A, Seguin C, Bens M, and Vandewalle A (2002) 11beta-

hydroxyprogesterone acts as a mineralocorticoid agonist in stimulating Na⁺ absorption in mammalian principal cortical collecting duct cells. *Mol Pharmacol* **62**:1306-1313.

Rafestin-Oblin ME, Souque A, Bocchi B, Pinon G, Fagart J, and Vandewalle A (2003) The

severe form of hypertension caused by the activating S810L mutation in the mineralocorticoid receptor is cortisone related. *Endocrinology* **144**:528-533.

Rossi G, Boscaro M, Ronconi V, and Funder JW (2005) Aldosterone as a cardiovascular risk

factor. *Trends Endocrinol Metab* **16**:104-107.

MOL 36459

- Souque A, Fagart J, Couette B, Davioud E, Sobrio F, Marquet A, and Rafestin-Oblin ME (1995) The mineralocorticoid activity of progesterone derivatives depends on the nature of the C18 substituent. *Endocrinology* **136**:5651-5658.
- Storoni LC, McCoy AJ, and Read RJ (2004) Likelihood-enhanced fast rotation functions. *Acta Crystallogr D Biol Crystallogr* **60**:432-438.
- Trapp T and Holsboer F (1995) Ligand-induced conformational changes in the mineralocorticoid receptor analyzed by protease mapping. *Biochem Biophys Res Commun* **215**:286-291.

MOL 36459

Footnotes

This work received funding from the Institut National de la Santé et de la Recherche Médicale (INSERM) and the European Symposium of the Aldosterone Council (ESAC).

Accession code. The Protein Data Bank ID code for the structure of MR_{S810L}-LBD associated with SC9420 is 2OAX.

MOL 36459

Legends for figures

Fig. 1. Structural formulae of spiro lactones.

Fig. 2. Effect of spiro lactones on the MR_{S810L} transactivation activity. HEK 293T cells transiently expressing MR_{S810L} were incubated for 24 h with increasing concentrations (10⁻¹¹ to 10⁻⁶ M) of aldosterone (ALDO), SC9420, RU26752, mexrenone (MEX) or canrenone (CAN). The transactivation activities of MR_{S810L} were determined from the luciferase activity normalized in terms of the β-galactosidase activity. Results are expressed as a percentage of MR_{S810L} activity in response to 10⁻⁹ M aldosterone. Values are mean ± S.E.M. of three separate experiments.

Fig. 3. Crystal structure of the MR_{S810L}-LBD associated with SC9420. (A) Stereo view of the 2Fo-Fc electron density map showing SC9420, and the surrounding residues in the MR_{S810L}-LBD. The map was calculated at 2.29 Å and contoured at 1 σ. This figure was produced using DINO (<http://www.dino3d.org>). (B) Diagram showing the interactions between MR_{S810L}-LBD and SC9420. Hydrogen bonds and van der Waals interactions are depicted as solid red arrows and dashed black lines, respectively. W indicates a water molecule.

Fig. 4. Ligand-binding pockets of MR_{S810L}-LBD associated with SC9420 (A) and progesterone (PDB ID 1YA3) (B). The ligand cavities volumes (grey) were calculated by VOIDOO (Kleywegt and Jones, 1994). This figure was produced using DINO (<http://www.dino3d.org>).

Fig. 5. Superimposition of the structure of the LBD of MR_{S810L} associated with SC9420 (blue) over that of MR_{WT}, associated with deoxycorticosterone (grey) (PDB ID 2ABI). (A) Overall

MOL 36459

organization of the LBDs. (B) focus on the ligand-binding cavities. Hydrogen bonds and van der Waals interactions are depicted as dashed green and black lines, respectively. This Figure was produced using DINO (<http://www.dino3d.org>).

Fig. 6. Spirolactones within the ligand-binding cavity of MR_{S810L}. (A) Superimposition of the minimized SC9420 (blue) over the SC9420 in the crystal structure (grey) within the ligand-binding cavity of MR_{S810L}. Docking of the lowest energy conformations of RU26752 (B) and mexrenone (C) within the ligand-binding cavity of MR_{S810L}. Van der Waals volumes of the C7 substituent are depicted in red, and those of Phe829 and Leu938 in black. The figure was generated using Open PyMol version 0.93.

Fig. 7. Transactivation properties of MR_{S810L/Q776A} and MR_{S810L/R817A} in response to spirolactones. HEK 293T cells transiently expressing MR_{S810L/Q776A} (A) and MR_{S810L/R817A} (B) were incubated for 24 h with 10⁻⁷ M of aldosterone in the absence (100% agonist activity) or presence of increasing (10⁻⁸ M to 10⁻⁵ M) concentrations of SC9420, RU26752, mexrenone (MEX) and canrenone (CAN). Transactivation activities of mutant MRs were determined from the luciferase activity normalized in terms of the β-galactosidase activity. Values are mean ± S.E.M. of three separate experiments.

Fig. 8. Transactivation properties of MR_{S810L/N770A} in response to spirolactones. (A) HEK 293T cells transiently expressing MR_{S810L/N770A} were incubated for 24 h with 10⁻⁷ M progesterone (P) or 10⁻⁷ M to 10⁻⁵ M of the spirolactones to be tested. Results are expressed as the percentage of the MR_{S810L/N770A} activity in response to 10⁻⁷ M progesterone. (B) HEK 293T cells transiently expressing MR_{S810L/N770A} were incubated for 24 h with 10⁻⁷ M progesterone in the absence (100% agonist activity) or presence of increasing (10⁻⁷ M to 10⁻⁵ M) concentrations of the spirolactones tested. Transactivation activities of MR_{S810L/N770A} were

MOL 36459

determined from the luciferase activity normalized in terms of the β -galactosidase activity.

Values are mean \pm S.E.M. of three separate experiments.

Fig. 9. Transactivation properties of MR_{WT} and MR_{N770A} in response to spiro lactones. HEK 293T cells transiently expressing MR_{WT} (A) or MR_{N770A} (B) were incubated for 24 h with 10^{-7} M of 18OVP in the absence (100% agonist activity) or presence of increasing (10^{-7} M to 10^{-5} M) concentrations of the spiro lactones tested. Transactivation activities of MRs were determined from the luciferase activity normalized in terms of the β -galactosidase activity. Values are mean \pm S.E.M. of three separate experiments.

MOL 36459

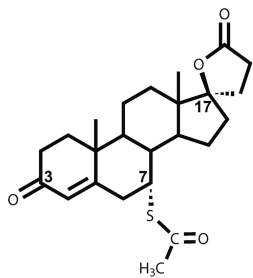
Table 1. Data collection and refinement statistics

MR_{S810L} - SC9420**	
Data collection	
Space group	P3 ₂
Cell dimensions	
<i>a, b, c</i> (Å)	122.20, 122.20, 91.81
α, β, γ (°)	90, 90, 120
Resolution (Å)	14.92 - 2.29 (2.43 - 2.29)*
<i>R</i> _{merge}	12.1 (62.3)*
<i>I</i> / σI	13.0 (2.66)*
Completeness (%)	91.1 (94.8)*
Redundancy	6.2 (5.65)*
Refinement	
Resolution (Å)	14.92 - 2.29
No. reflections	62950
<i>R</i> _{work} / <i>R</i> _{free}	24.0 / 26.3
No. atoms	
Protein	11503
Ligand/ion	174
Water	339
<i>B</i> -factors	
Protein	42.3
Ligand/ion	27.9
Water	39.9
R.m.s deviations	
Bond lengths (Å)	0.014
Bond angles (°)	1.2

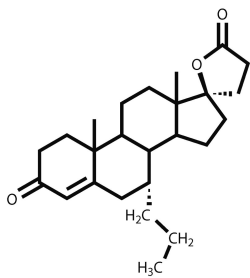
** One crystal was used to collect the data.

* Highest resolution shell is shown in parenthesis.

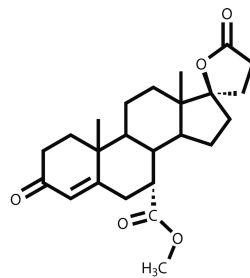
Fig. 1



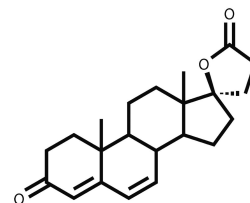
SC9420



RU26752



Mexrenone



Canrenone

Fig. 2

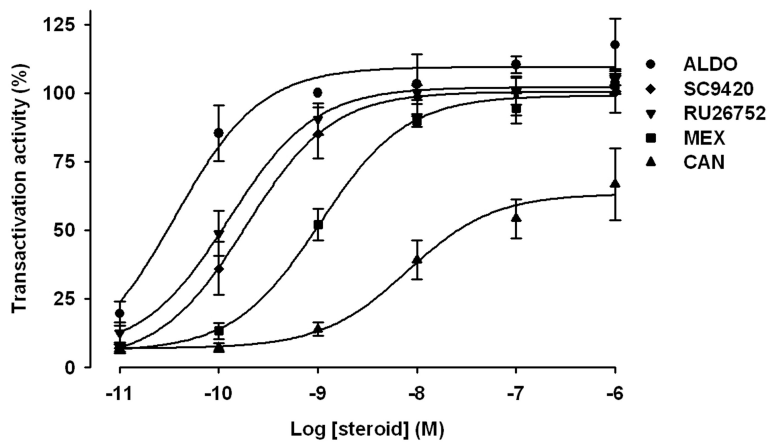


Fig. 3

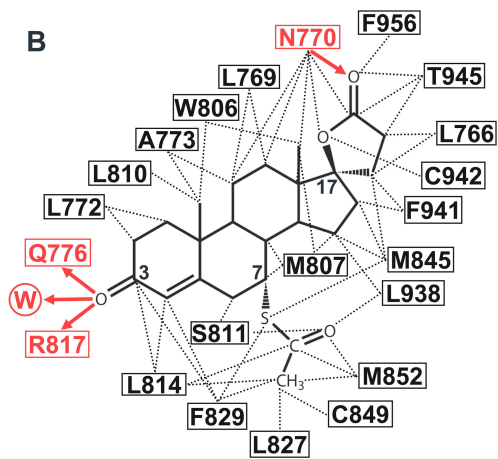
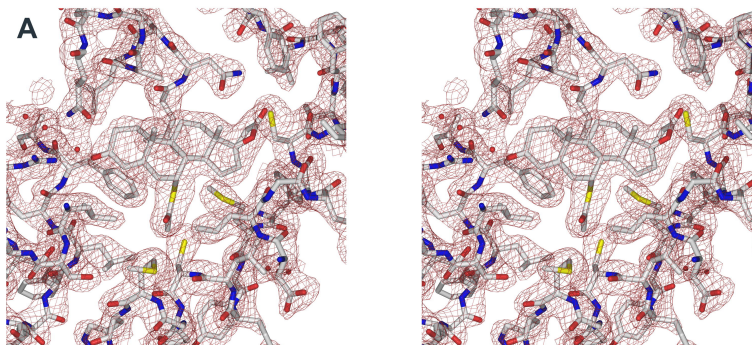


Fig. 4

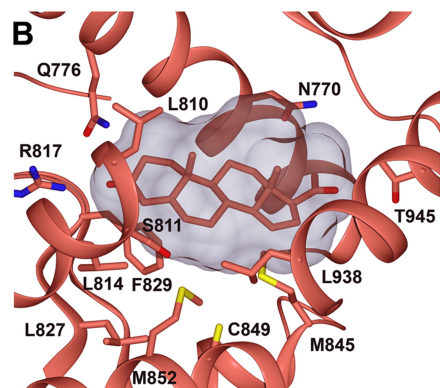
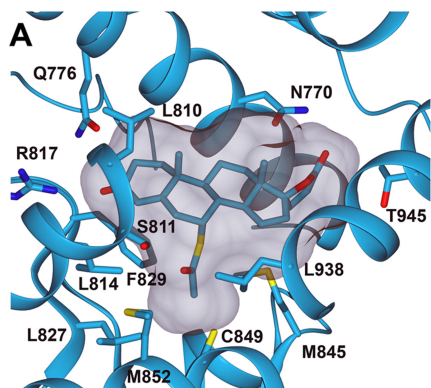


Fig. 5

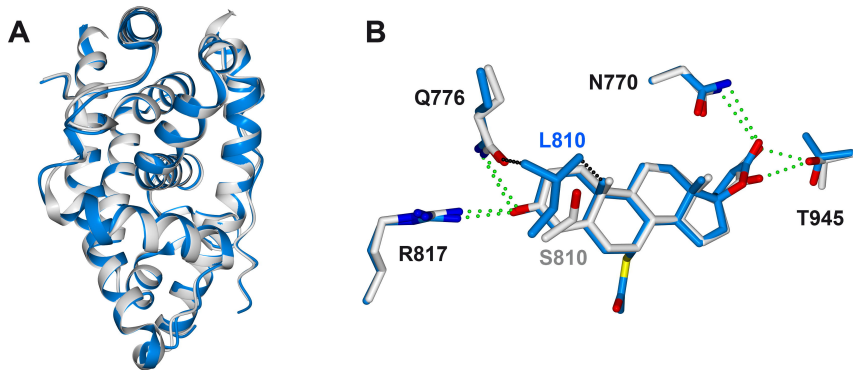


Fig. 6

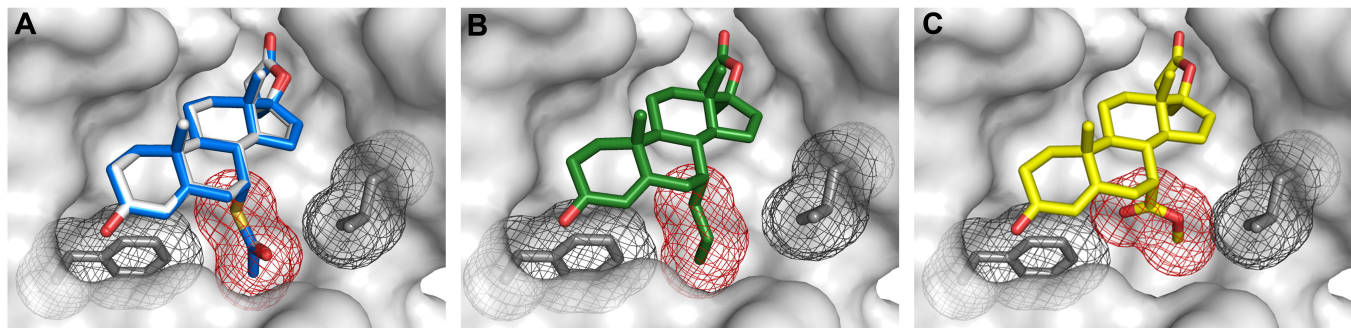


Fig. 7

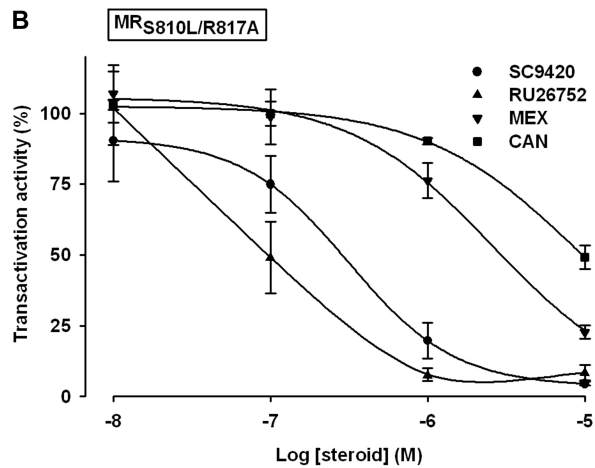
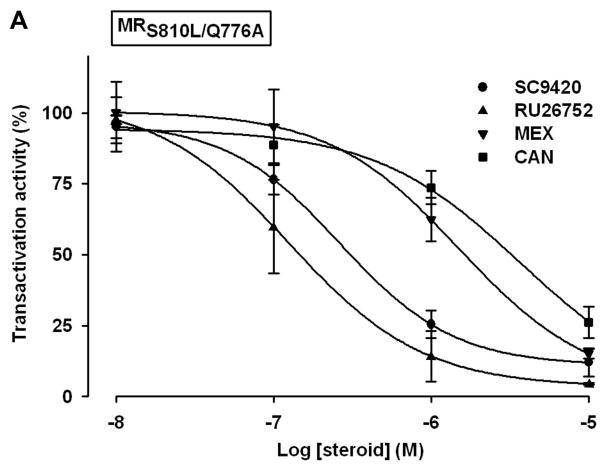


Fig. 8

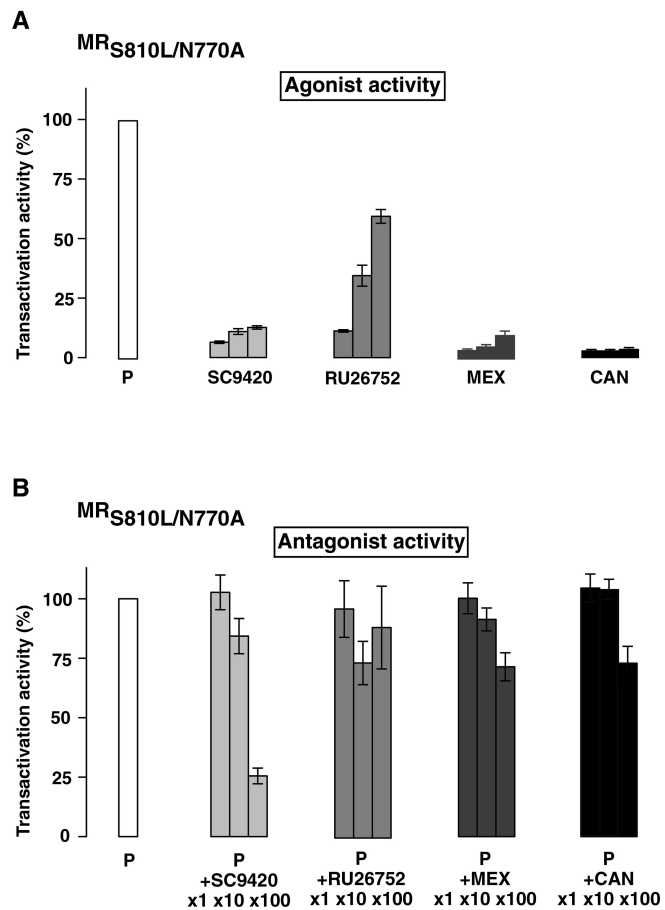


Fig. 9

